*Journal of Machine Engineering, Vol. 11, No. 4, 2011*

*control, machine tool,*
*angular thermal error,*
*transfer function*

Martin MARES[1]
Otakar HOREJS[1]
Jan HORNYCH[1]
Peter KOHUT[1]

# COMPENSATION OF MACHINE TOOL ANGULAR THERMAL ERRORS USING CONTROLLED INTERNAL HEAT SOURCES

Thermal errors caused by the influence of internal and external heat sources in machine tool structure can cause up to 70% of total machine tool inaccuracy. Therefore, research on thermal behavior of machine tool structures is crucial for successful manufacturing. This paper provides an insight into the modeling of highly nonlinear (increasing with the complexity of the structure) machine tool thermal behavior using thermal transfer functions. This approach to modeling is dynamic (uses thermal history) and, due to its relative simplicity, it enables real-time calculations. The method uses very few additional gauges and solves separately each influence participating in the thermal error. The main objective of the article is to describe the estimation of angular deformations occurring at the tool center point due to thermal influences. Transfer functions are used for the identification and control of additional internal heat sources. The second aim is to compare modeling effort with approximation quality. A partial objective is to cover other nonlinearities occurring generally in machine tool thermal behavior. The approach has been verified on a closed quill (a simple and symmetrical machine tool part) and applied on a model of a machine tool structure which has been chosen as the least favorable from the thermal point of view.

## 1. INTRODUCTION

Requirements for machining accuracy have increased significantly over the last several decades. Therefore, research on the temperature behavior of the machine tool (MT) structure is necessary for high-quality production. Thermal errors caused by internal (motors, drives, bearings, ball screws and their nuts, gear box etc.) and external heat sources (effect of the environment, machine operator, radiation etc.) can cause more than 50% of MT total error [1]. Different approaches exist to compensate for these errors. In general, it is possible to divide the thermal error issue into four groups [1-2]: MT structure enhancement aiming to obtain a thermally symmetrical structure, high-cost

[1] Research Center of Manufacturing Technology of the Czech Technical University in Prague, Horská 3, 12800, Prague Czech Republic, M.Mares@rcmt.cvut.cz, O.Horejs@rcmt.cvut.cz, J.Hornych@rcmt.cvut.cz, P.Kohut@rcmt.cvut.cz

Table 1. List of symbols

| Symbol | Quantity | Units |
|---|---|---|
| $y(t)$, $y(k-n)$ | output vector | |
| $u$, $u(t)$, $u(k-n)$ | input vector | |
| $\gamma$, $\gamma_i$ | DTF time domain | $\mu m/W$ |
| $\gamma^{-1}$, $\gamma_i^{-1}$ | Inversive DTF time domain | $W/\mu m$ |
| $\varepsilon$, $\varepsilon_i$ | TDTF time domain | $\mu m/°C$ |
| $Z$ | Integer delay | $s$ |
| $a_i$ | Weight factors of DTF input | $\mu m \cdot s^i/W$ |
| $b_i$ | Weight factors of DTF output | $s^i$ |
| *Fit* | Value of approximation quality | % |
| *Imp* | Value of improvement in relation to uncompensated state | % |
| $a_n$ | Lower boundary of validation of n$^{th}$ DTF | *rad* |
| $b_n$ | Upper boundary of validation of n$^{th}$ DTF | *rad* |
| $Y$ | Vector of measured values | |
| $Y_{HAT}$ | Vector of simulated values | |
| $\bar{Y}$ | Arithmetic mean of elements of the measured values vector | |
| $\bar{Y}_{HAT}$ | Arithmetic mean of elements of the simulated values vector | |
| $error_\delta$ | Approximation error of linear thermal deformations | $\mu m$ |
| $error_Q$ | Approximation error of heat source power | $W$ |
| $error_\varphi$ | Approximation error of angular thermal deformations | $W$ |
| $\varphi_x$ | Calculated angular deformation: $\varphi_x = (\delta_{x2} - \delta_{x1}) / \Delta$ | *rad* |
| $\varphi_C$ | Angular deformation caused by causal heat source | *rad* |
| $\varphi_S$ | Angular deformation caused by stabilization heat source | *rad* |
| $Q_C$ | Causal heat source power | $W$ |
| $Q_S$ | Stabilization heat source power | $W$ |
| $\Delta T$ | Measured temperature difference | $°C$ |
| $\delta_{x1}$ | Measured linear deformation $x_1$ | $\mu m$ |
| $\delta_{x2}$ | Measured linear deformation $x_2$ | $\mu m$ |
| $\delta_z$ | Measured linear deformation z | $\mu m$ |
| $\delta_m$ | Measured linear deformation TCP generally | $\mu m$ |
| $\delta_C$ | Straight deformation caused by causal heat source | $\mu m$ |
| $\delta_S$ | Linear deformation caused by stabilization heat source | $\mu m$ |
| $\Delta$ | Distance between displacement probes in *x* direction | *mm* |

materials with low values of thermal expansion coefficient [3]; control of the heat flux (e.g. control of MT cooling system [4], heat pipes [5] etc.); direct compensation (measurements between the tool and workpiece, e.g. laser beam [2]); or **indirect compensation** (mathematical models).

A transfer function (TF) describes the connection between outputs (response) and inputs (excitement) of a dynamic system in the frequency domain. Deformational transfer functions (DTF) and temperature-deformational transfer functions (TDTF), express the connection between a heat source, or temperature close to a heat source, and one-point-deformation caused by thermal expansion [6]. The modeling of thermo-mechanical systems by using TDTFs is rapid (and so suitable for real-time applications), dynamic (unlike the most widespread compensation method based on multiple regression analysis, the model considers the thermal history of the MT [7]), needs only few temperature probes in comparison with e.g. artificial neural networks (ANN) [8], and provides quality comparable to time-consuming methods such as finite element analysis (FEM) [9]. Moreover, TDTF compensation allows for solving various thermal behavior nonlinearities separately without the need for additional gauges.

A similar mathematical approach was also used in [10]. However, NC data such as spindle speed and effective power were used as input for the estimated transfer functions in this case. Another research topic addressed by the authors of [10] was the compensation of thermo-dependent MT deformations due to spindle load [11-12]. Here, a combination of direct and indirect compensation was employed to reduce modeling effort. However, this makes the method less accurate.

The efficiency of the mathematical approach using TDTFs (where temperatures have been used as input for the transfer function) has been successfully verified on a quill model (a simple symmetrical machine tool component) [13], as well as on a real MT structure [14]. The main objective of this article is to predict the TF of angular deformations occurring at the tool center point (TCP) due to thermal influences. The second aim is to compare modeling time intensity with approximation quality. A partial objective is to cover other nonlinearities occurring generally in machine tool thermal behavior (approximation of linear error in $x$, $y$ and $z$ through TDTFs superposition). The approach has been verified on a closed quill [15], and applied on a model of a machine tool structure (so-called ‘C-frame’) which has been chosen as the least favorable from the thermal point of view.

## 2. ANALYSIS OF THERMAL BEHAVIOUR AND THE MATHEMATICAL APPROACH

All data processing and TF identification, as well as quill and C-frame thermal behavior modeling and verification, were performed in *Matlab* and *Matlab simulink*. Data recording, along with the implementation of thermo-elastic models as a control system, were performed with *National Instruments* diagnostic devices and *LabVIEW*.

### 2.1. MATHEMATICAL APPROACH

A discrete 2$^{nd}$ order TF was used to describe the link between the excitation and its response. The differential form of the TF in the time domain is introduced in (1):

$$y(k)=\frac{u(k-1)a_1+u(k)a_0+y(k-2)b_2+(k-1)b_1}{b_0}, \tag{1}$$

where $k$-$n$ means the $n$-multiple delay. Linear parametric models of ARX (autoregressive with external input) or OE (output error) identifying structures were used

[16]. The quality of each TDTF was examined through linear time invariant (LTI) step response [14],[16].

The approximation quality of the simulated behavior is expressed by the *fit* (*%*) value (2):

$$fit = \left( \frac{\left\| Y - Y_{HAT} \right\|}{\left\| Y - \bar{Y} \right\|} \right) \cdot 100 \qquad (2)$$

Charts showing the approximation model include an improvement (%) value (3), compared to an uncompensated state:

$$imp = 100 - \frac{100 \cdot \left| \bar{Y}_{HAT} \right|}{\left| \bar{Y} \right|} \qquad (3)$$

The error of approximation is expressed as shown in Eq.(4). It also represents the fictitious deformation obtained after implementing the model in the control system.

$$error = Y - Y_{HAT} \qquad (4)$$

### 2.2. THERMAL BEHAVIOR - BASIC MODEL

The basic model describing thermal angular deformations was implemented on a quill for its simplicity and clarity. Two electric heaters were placed asymmetrically on the quill surface. The first heater simulated a causal heat source responsible for undesirable angular deformations, while the second was used as a stabilization heat source, as shown in Fig. 1 (left). A diagram showing the deformation response measurement on the fictitious tool is depicted in the same picture (right). Three contactless displacement probes were used. The distance between the probes in the *x* direction was *Δ = 100 mm*. Only two thermal probes placed close to the heat sources were sufficient for the prediction of thermal angular errors.

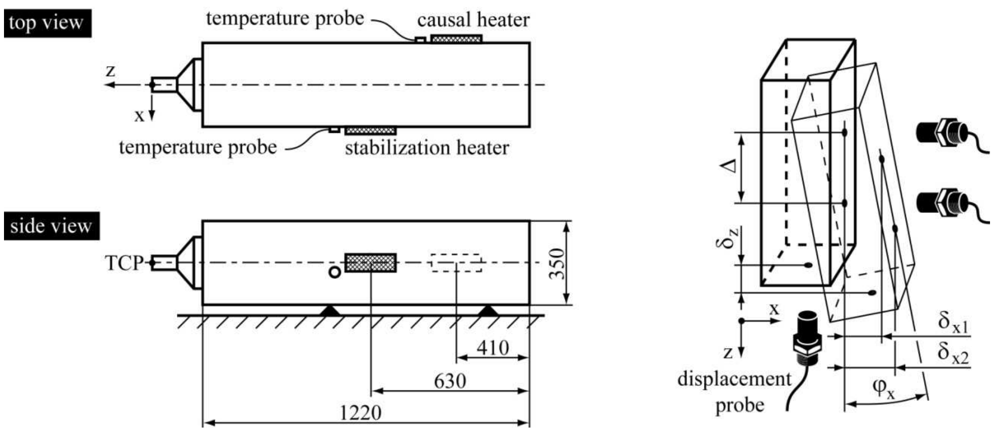


Fig. 1. Quill diagram (left) and deformation response measurement setup on a fictitious tool (right)

It is possible to compile the basic equation of thermal angular error approximation (6) from the basic condition of equality between the causal and stabilization heaters (5):

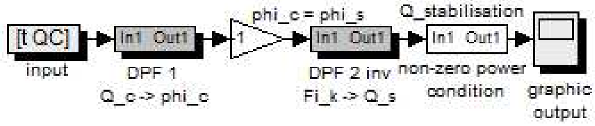


$$|\varphi_C| = |\varphi_S|\,, \tag{5}$$

$$Q_S = \underbrace{\left(Q_C \cdot \gamma_1\right)}_{\varphi_C} \cdot \gamma_2^{-1}\,. \tag{6}$$

Linear deformations are then expressed as a sum of causal and stabilization heat source elements (7). The equation is validated for both the *x* and *z* directions (*y* is neglected):

$$\delta_m = \underbrace{\Delta T_{Cm} \cdot \varepsilon_1}_{\delta_C} + \underbrace{\Delta T_{Sm} \cdot \varepsilon_2}_{\delta_S}\,. \tag{7}$$

Two calibration measurements were necessary to obtain all information required to build a basic thermo-elastic model. The value of 90 W was applied as the heat source power ($Q_C$) during calibration measurements on the causal heater. The measurements were conducted until the quill reached a thermally steady state. DTF $\gamma_1$ (response $\varphi_C$ to excitation $Q_C$) and TDTF $\varepsilon_1$ (response $\delta_C$ to excitation $T_{Cm}$) were obtained from this calibration measurement, as depicted in Fig. 2. Similar measurements were performed on the stabilization heater. The DTF $\gamma_2^{-1}$ (response $Q_S$ to excitation $\varphi_S$) and TDTF $\varepsilon_2$ (response $\delta_S$ to excitation $T_{Sm}$ ) were obtained from a second calibration measurement, depicted in Fig. 3. From identification purposes it was necessary to start from the zero value for excitation and response. This is the reason why the symbol $\Delta T_m$ is used in the figures.

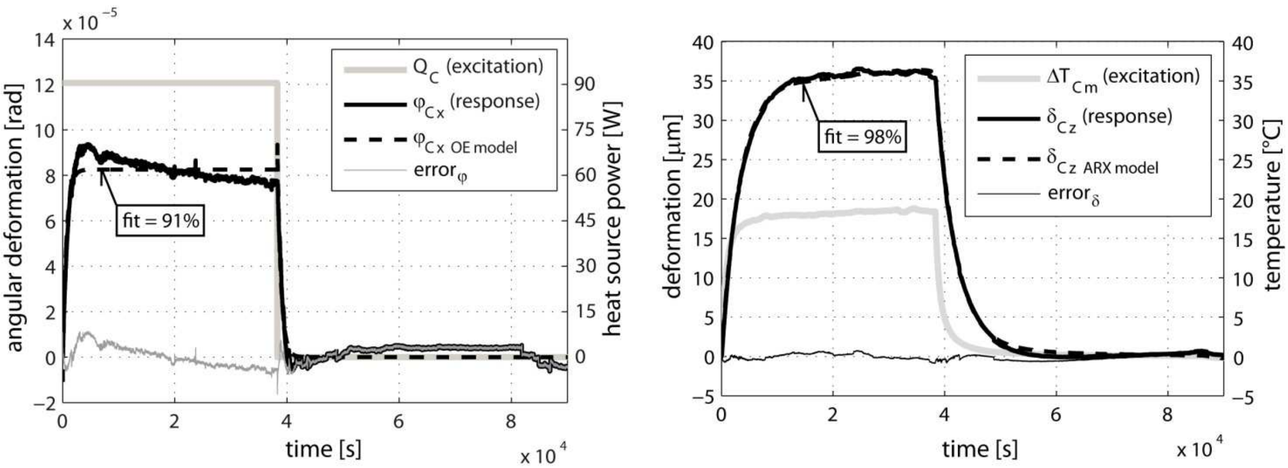


Fig. 2. Calibration measurement and identification of DTF (left) and TDTF (right) for causal heater

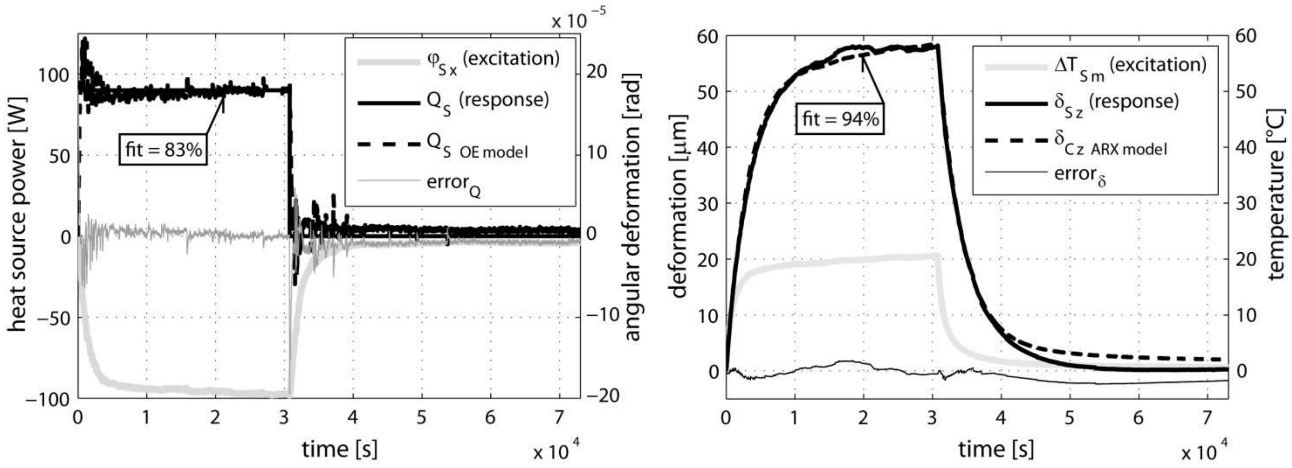


Fig. 3. Calibration measurement and identification of DTF (left) and TDTF (right) for stabilization heater

The results of the basic thermo-elastic model of the quill are shown in Fig. 4. The comparison of the causal and stabilization heat source power and the difference between the data measured with and without compensation, according to Eq. (3) a (4), are depicted in the left-hand part of Fig. 4. The linear error in the *z* direction, calculated according to Eq. (7), is shown on the right. The compensation of linear deformations in other axes is either similar or negligible. With the compensation heater applied, the angular deformations of the quill due to the effects of temperature decreased from the original $9.10^{-5} rad$ to $2.10^{-5} rad$ (improvement of approximately *78%*) in the *x* direction. Linear deformations decreased from $60\mu m$ to $4\mu m$ (improvement of approximately *95.5%*) in the *z* direction.

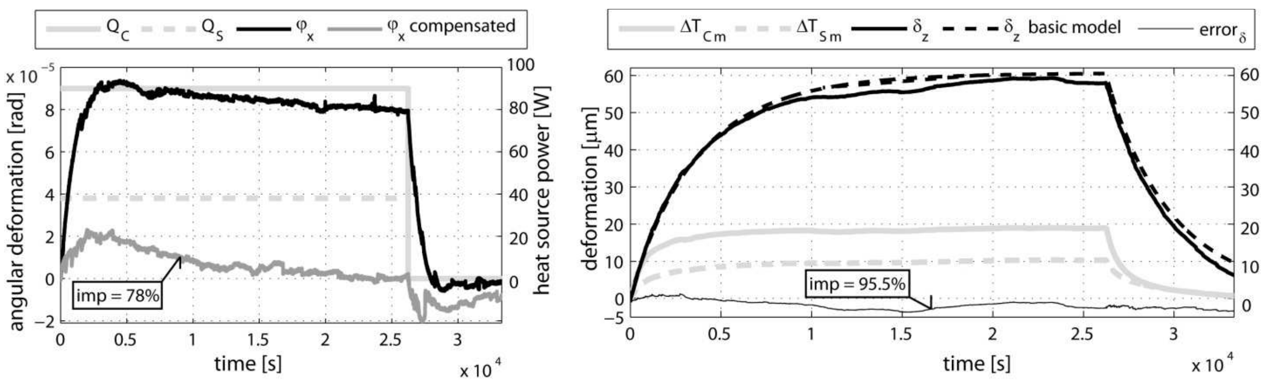


Fig. 4. Comparison of quill measurements with and without compensation

## 3. C-FRAME MODELS

An experimental test bed (so-called C-frame) with an asymmetrical thermal structure, corresponding to the most complicated thermo-elastics in practice, was created for the purposes of advanced experiments and attempts to simulate a real MT structure (Fig. 5.).

Two heaters were placed asymmetrically on the surface of the C-frame, as shown in Fig. 5. The power of both the causal and the stabilization heaters was adjusted to *70W* during calibration experiments. The reading of displacement and the determination of angular deformations corresponded to the diagram in Fig. 1. The distance between the probes in the *x* direction was $\Delta = 200\ mm$. Two temperatures were again sufficient for the description of the thermo-elastic behavior at the TCP of the C-frame. The power of both heat sources was controlled by a dimmer.

Figures showing the results of calibration measurements are not included due to their close resemblance to Fig. 2 and Fig. 3. The *fit* values obtained through identification are summarized in the following table.

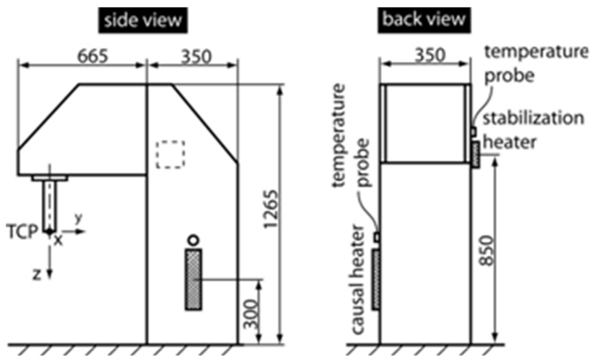


Fig. 5. Scheme of C-frame and experiment set-up

Tab. 2. Fit values of calibration measurements

| PF name | Causal heater | | | Stabilization heater | | |
|---|---|---|---|---|---|---|
| | $\gamma_1$ | $\varepsilon_{1z}$ | $\varepsilon_{1x}$ | $\gamma_2^{-1}$ | $\varepsilon_{2z}$ | $\varepsilon_{2x}$ |
| **Excitation** | $Q_C$ | $\Delta T_{mC}$ | $\Delta T_{mC}$ | $\varphi_C$ | $\Delta T_{mS}$ | $\Delta T_{mS}$ |
| **Response** | $\varphi_C$ | $\delta_{Cz}$ | | $Q_S$ | $\delta_{Sz}$ | |
| **Fit value** | 95% | 98% | 98% | 95% | 99% | 96% |

## 3.1. CORRECTED MODEL

The drawbacks of the basic thermo-elastic model are caused by nonlinear dependence between the heat source power and the measured angular deformation. This nonlinearity is caused, first of all, by including voltage regulators in the control loop of the C-frame thermal behavior. Two additional measurements—in a suitably chosen power *spectrum A*—were performed in order to demonstrate and correct nonlinearity. A thermal steady state needed to be reached in each power step of the chosen *spectrum A*.

It was possible to replace the causal heat source power input with the temperature measured close to the heat source, the dependence on angular thermal deformation being linear in this case. The relevant TDTF $\varepsilon_3$ was obtained from calibration measurements of the causal heater (*fit = 96%*). The result of this correction is depicted in the following Figure.

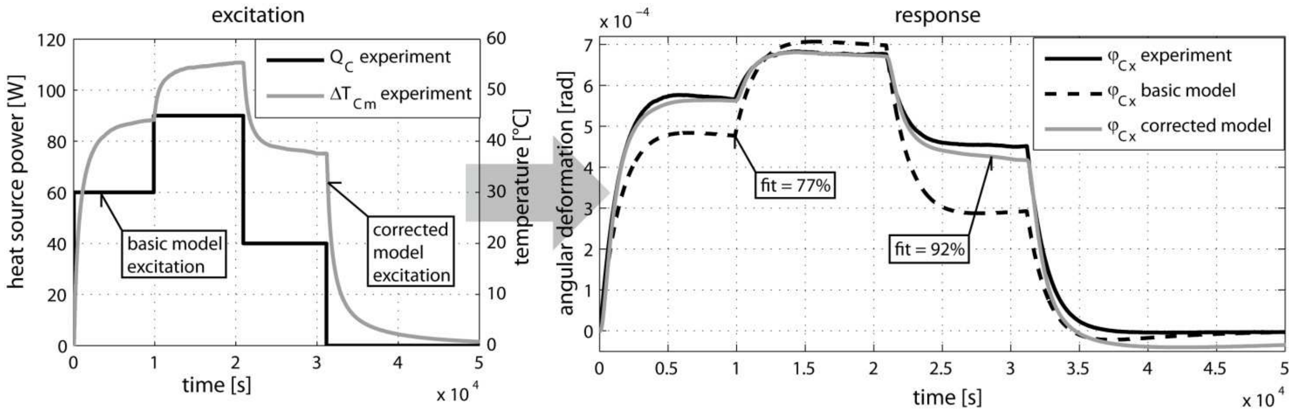


Fig. 6. Correction of causal heater

The situation is quite complicated in the case of the stabilization heater. There is no option for controlling the thermal deformation, except using the power of the heater with the nonlinear dependence. A correction polynomial had to be calculated. The value of $Q_S$ obtained from the basic model, multiplied by the polynomial, covers the behavior mentioned. The results are shown in Fig. 7.

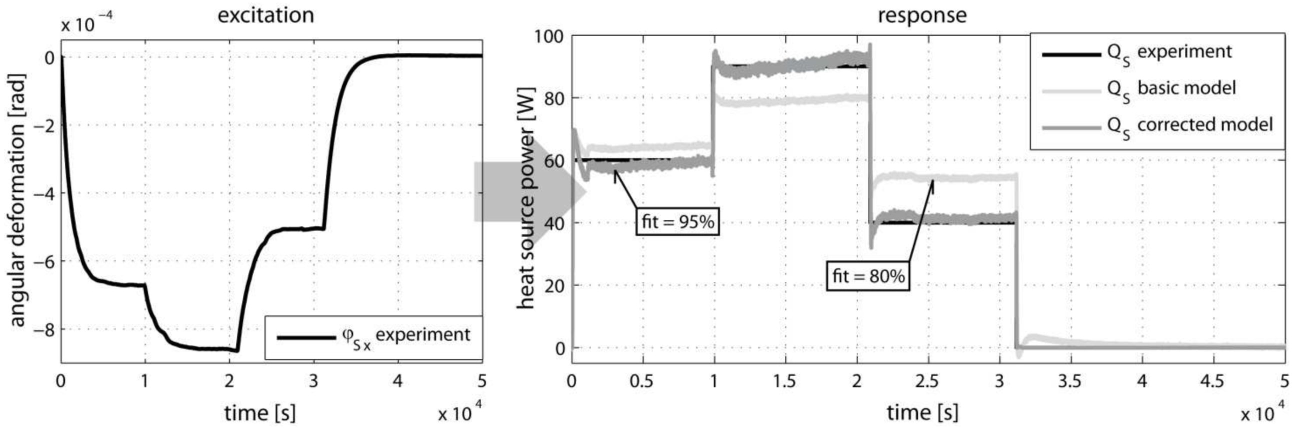


Fig. 7. Correction of stabilization heater

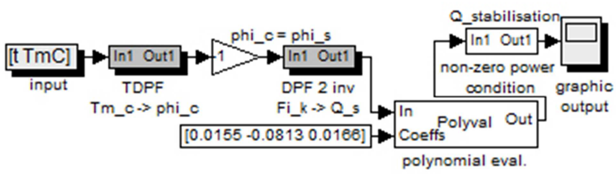


$$Q_S = \underbrace{\left(\Delta T_{mC} \cdot \varepsilon_3\right)}_{\varphi_C} \cdot \gamma_2^{-1} \cdot \underbrace{p^{(n)}\left(Q_S, \varphi_S\right)}_{correction\ function}, \qquad (8)$$

where the correction function is a 2nd order polynomial:

$$p = 0.0155 \cdot u^2 - 0.0813 \cdot u + 0.0166\,. \qquad (9)$$

The corrected thermo-elastic model of the C-frame is expressed by Eq.(8). The basic condition from Eq. (5) also has to be validated in this model.

### 3.2. MULTIPLE MODEL

Another approach to the modeling of thermal angular errors in MT is possible, although the solution using a corrected model is satisfactory. It is possible to divide the power range of the stabilization heater into several subgroups, each with its own DTF. The choice of a suitable DTF is related to the simulated value of angular deformations originating from the causal heater as shown in condition (10).

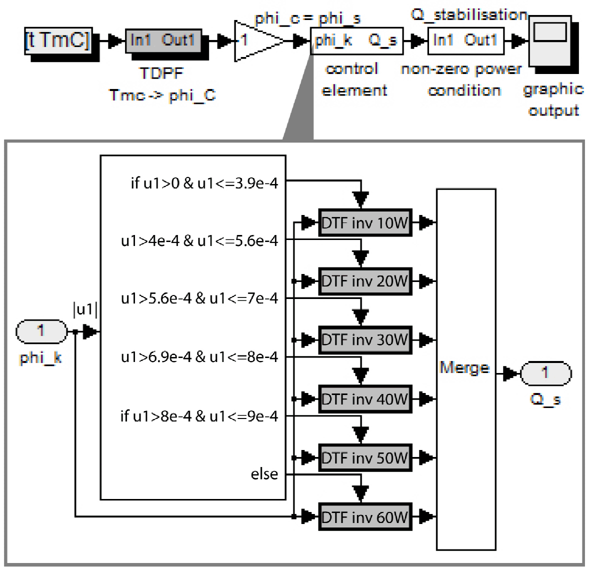


$$|\varphi_C| > a_n \wedge |\varphi_C| > b_n \qquad (10)$$

The formula validated for the determination of the stabilization heat power is then as follows:

$$Q_S = \underbrace{(\Delta T_{mC} \cdot \varepsilon_3)}_{\varphi_C} \cdot \gamma_n^{-1} \quad \text{where } n = 3 \ldots 8. \qquad (11)$$

The power range of the stabilization heater was divided into six groups in *10W* increments. The necessary calibration measurements and the comparison with the efficiency of other models are depicted in Fig. 8. The *fit* values of the DTFs identified are summarized in Table 3.

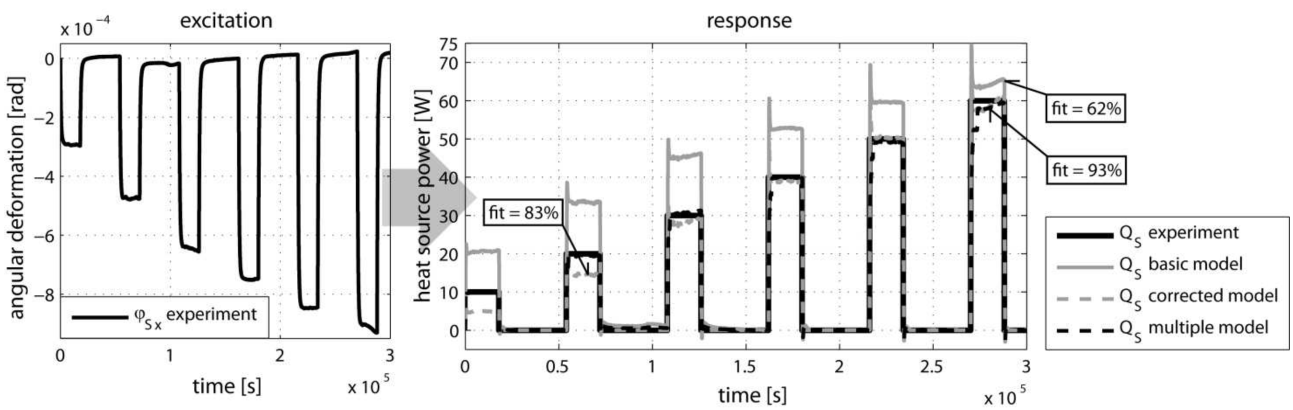


Fig. 8. Additional calibration measurement of stabilization heater

Tab. 3. Fit values of accessory calibration measurements

| DTF name | Stabilization heater | | | | | |
|---|---|---|---|---|---|---|
| | $\gamma_3^{-1}$ | $\gamma_4^{-1}$ | $\gamma_5^{-1}$ | $\gamma_6^{-1}$ | $\gamma_7^{-1}$ | $\gamma_8^{-1}$ |
| **Response** [W] | 10 | 20 | 30 | 40 | 50 | 60 |
| **Fit value** | 93.5% | 89% | 93.5% | 93.5% | 93% | 92% |

## 4. COMPENSATION RESULTS

The results of the basic thermo-elastic model [Eq.(6)], corrected thermo-elastic model [Eq.(8)] and multiple model [Eq.(10) and (11)], applied to the power *spectrum A* (set on the causal heater) are depicted in Fig. 9. The values expressing the improvement of the model in relation to an uncompensated state are presented in the figure. The compensation results for thermal angular deformations are printed in the left-hand part of the picture, and the compensation of linear deformations in both the *x* and *z* directions, in the right-hand part. Linear deformations in the *y* direction are negligible.

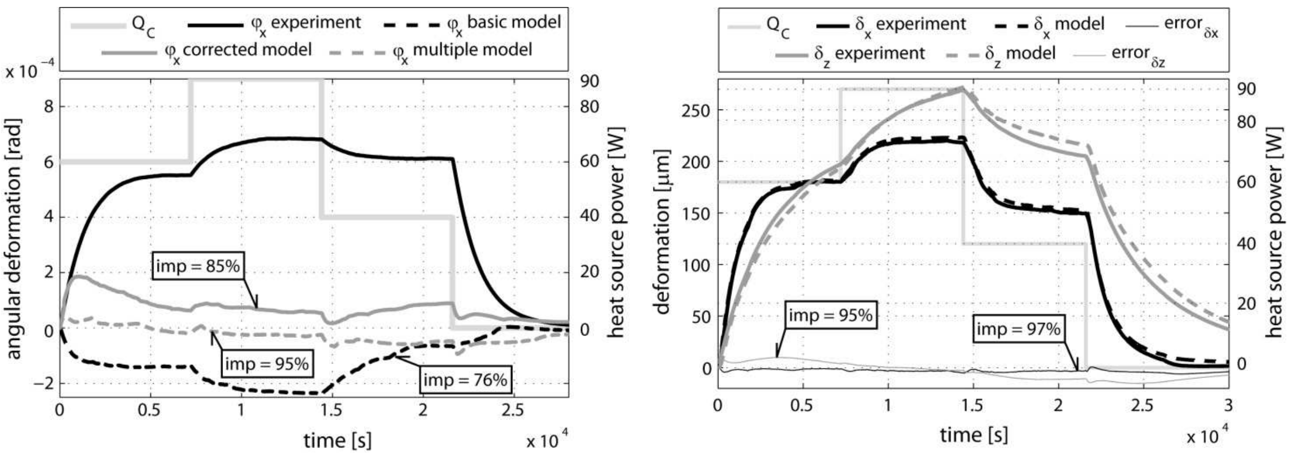


Fig. 9. Compensation results of spectrum A

Two calibration measurements (one for each heater) lasting approximately 24 hours were necessary to compile the basic thermo-elastic model of the C-frame. Under the conditions determined by the power *spectrum A* of the heat source, the basic model achieved an improvement of *76%* in relation to an uncompensated state of thermal angular deformations in the *x* direction.

One additional calibration measurement of the stabilization heater was performed in order to correct the deficiencies of the previous model. The calibration measurement served to compute a correction polynomial. The total number of calibration measurements needed to obtain a corrected thermo-elastic model of the C-frame is three (36 hours in duration). The corrected model reaches an improvement of *85%* in relation to an uncompensated state.

The deficiency of the corrected model consists in the poor quality of the description of the transitional phases between the individual heat power steps. It is the role of the multiple thermo-elastic model of the C-frame, consisting of six inverse DTFs, to compensate for the deficiency. These six inverse DTFs describe the nonlinear thermal behavior of the stabilization heater. This nonlinearity is caused, first of all, by the inclusion of voltage regulators into the control loop of the C-frame thermal behavior. The number of calibration measurements is equal to seven (one for the causal heater and six for the stabilization heater), approximately 84 hours in duration. The multiple model achieves an improvement of *95%* in relation to an uncompensated state.

## 5. CONCLUSIONS

This article describes an effective approach to the compensation of thermal angular deformations, consisting in the use of controlled internal heat sources, *Matlab* tools and thermal TFs [6] on a MT model with an asymmetrical temperature structure (C-frame), using a minimum of additional gauges. The experiment set-up consisted of two asymmetrically placed heaters: one as a causal thermal source causing angular deformations, and a second one used for stabilizing these deformations. The first aim of the paper has been to build a basic approximation thermo-elastic model of a quill, and then apply the model on a C-frame structure. The thermo-elastic model also contains an approximation of linear deformations occurring generally in MT thermal behavior.

Two additional variations of the C-frame thermo-elastic model, accounting for different corrections to the description of nonlinearities caused by inserting voltage regulators into the control loop of the heater, have been designed. The second aim has been to compare modeling time intensity with model approximation quality.

All of the thermo-elastic models of the C-frame have been verified using a test with changeable causal heat source power (power spectrum). The results for the models are shown in Table 4. The results from the random power *spectrum B* (Fig. 10.) are given in Table 4, in addition to the results from the simpler *spectrum A* (see Chapter 4 above).

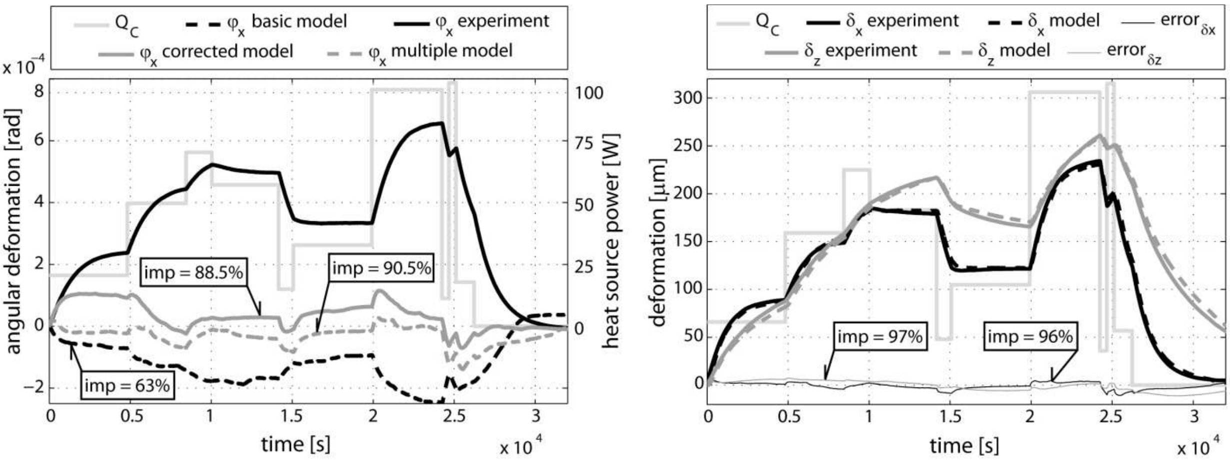


Fig. 10. Compensation results for spectrum B

Tab. 4. Comparison of thermal angular error approximation results for the C-frame

| **Thermo-elastic model** | **Improvement value** [%] | | **No. of calibration measurements** | **Time consumption** [hours] |
|---|---|---|---|---|
| | **Spectrum A** | **Spectrum B** | | |
| **Basic** | 76 | 63 | 2 | 24 |
| **Corrected** | 85 | 88.5 | 3 | 36 |
| **Multiple** | 95 | 90.5 | 7 | 84 |

The multiple thermo-elastic model has proved to be valid from the point of view of approximating the transitional phase between two power steps. However, all three models have their deficiencies related to the description of angular deformations occurring during quick changes in the causal heat source power (see the very end of *spectrum B* – Fig. 10.). Therefore, the usability of the multiple thermo-elastic model is a matter for consideration, given the high modeling effort and the little improvement provided by the polynomial-corrected model. The basic model is not sufficient for compensating thermal angular deformations of more complicated and thermally asymmetrical structures, such as a C-frame, despite the results obtained from the quill application and the low modeling effort.

The application and testing of the model on a real MT is the main objective of further research. However, additional experiments and reflections should be carried out to take account of more influences, such as tool positioning in the work-space (the model is calibrated for one position, in line with the majority of other known and available models), to take heat transfer coefficient into consideration, and to include the influences of more than one heat source.

## REFERENCES

[1] WECK M., MCKEOWN P., BONSE R., HERBST U., 1995, *Reduction and compensation of thermal errors in machine tools*, Annals of the CIRP, 44/2/589-598.

[2] RAMESH R., MANNAN M. A., POO A. N., 2000, *Error compensation in machine tools - a review, Part II: thermal errors*, in International Journal of Machine Tools & Manufacturing, 40/1257 -1284.

[3] MEO F., MERLO A., RODRIGUEZ M., BRUNNER B., FLECK N. A., LU T. J., MAI S. P., SRIKANTHA PHANI A., WOODHOUSE J., 2008, *Advanced hybrid mechatronic materials for ultra precise and high performance machining system design. Innovative production machines and systems*, D.T. Pham, E.E. Eldukhri and A.J. Soroka (eds), MEC. Cardiff University, UK.
[4] HORNYCH J., BARTA P., HOREJS O., VYROUBAL J., 2007, *Thermal transfer function based control of a machine tool cooling system*, In proceedings of the topical meeting: Thermal Effects in Precision System. Maastricht, Netherlands, 18 - 19.
[5] BORUNDIA A., TRAN H. D., 2002, *An experimental investigation of heat pipes at low power inputs,* in proceedings of the ASPE 17th annual meeting.
[6] BARTA P., 2008, *Frequency transfer functions in thermo-mechanics*, doctoral thesis, Czech Technical University in Prague, Faculty of Mechanical Engineering, 83.
[7] TSENG P.-C., 1997, *A real-time inaccuracy compensation method on a machining centre*, The International Journal of Manufacturing Technology 13, Springer-Verlag London Ltd., 182-190.
[8] LEE J., KRAMER B. M., 1993, *Analysis of machine degradation using a neural network based pattern discrimination model*, Journal of Manufacturing Systems, 12/5/379-387.
[9] SHAUNGHUI H., LIU J., SONG B., HAO M., ZHENG W., TANG Z., 1999, *Research on thermal error of the 3D-coordinate measuring machine based on the finite element method*, ICIRA, Part II, LNAI 5315, 440-448.
[10] BRECHER C., HIRSCH P., 2004, *Compensation of thermo-elastic machine tool deformation based on control internal data*, in annals of the CIRP, 53/1/299 - 304.
[11] BRECHER C., WISSMANN A., KLEIN W., 2010, *Compensation of thermo-dependent machine tool deformations due to spindle load based on reduced modelling effort*, in 14th International Conference on Mechatronic Technology (ICMT), Osaka, Japan, 295 - 302.
[12] BRECHER C., WISSMANN A., KLEIN W., 2010, *Compensation of thermo-dependent machine tool deformations due to spindle load based on reduced experimental procedure modelling effort-synthesis between direct and indirect compensation*, in: 8h International Conference on High Speed Machining, www.enim.fr/hsm2010, Metz, France, 8.
[13] MARES M., BARTA P., 2008, *Mechatronic approach in modelling, identification and control of thermal deformation of quill*, MM Science Journal, 10/25 – 29.
[14] MARES M., HOREJS O., KOHUT P., HORNYCH J., BARTA P., 2010, *Application of mechatronic approach to modelling, identification and control of machine tool thermal errors*, in proceedings of the 29th IASTED International Conference: Modelling, Identification and Control (MIC 2010), Innsbruck, Austria, 284-290.
[15] MARES M., 2010, *Kompenzace teplotních úhlových deformací pinoly pomocí řízených vnitřních zdrojů tepla,* Konference studentské tvůrčí činnosti (STČ 2010), Praha, http://stc.fs.cvut.cz, 10 s.
[16] LJUNG L., 2009, *System identification toolbox 7 User's guide*, www.mathworks.com (The MathWorks).